Synchrotron emission from relativistic parsec-scale jets.

A. R. Beresnyak^{1*}, Ya. N. Istomin^{1†} and V. I. Pariev^{1,2}

¹P. N. Lebedev Physical Institute, Leninsky Prospect 53, Moscow 117924, Russia

1 July 2018

ABSTRACT

We developed theory of particle acceleration inside the relativistic rotating electronpositron force-free jet with spiral magnetic field. We considered perturbation of stationary magnetic field structure and found that acceleration takes place in the regions where the Alfvén resonant condition with the eigenmodes in the jet is fulfilled, i.e. where the local Alfvén speed is equal to the phase speed of an eigenmode. Acceleration process and synchrotron losses combined together form power law energy spectrum of ultrarelativistic electrons and positrons with index between 2 and 3 depending upon initial energy of injected particles. Synchrotron emission of these electrons and positrons in spiral magnetic field of rotating force-free jet has been calculated. Polarization properties of the radiation has been obtained and compared with existing VLBI polarization measurements of parsec-scale jets in BL Lac sources and quasars. Our results give natural explanation of observed bimodality in alignment between electric field vector and jet axis. Degree of polarization and velocity of observed proper motion of bright knots depend upon angular rotational velocity of the jet. Thus, comparing them to each other, we can estimate angular rotational velocity in jets. These results indicate that the fact, that generally in BL Lac objects electric field vector is oriented parallel to the jet axis while in quasars perpendicular to the jet axis, may be due to intrinsically larger angular rotational velocity and large winding of magnetic field in BL Lac jets than in quasar jets.

Key words: radiation mechanisms:nonthermal – magnetic fields – plasmas – galaxies:jets.

1 INTRODUCTION

The nature of the Active Galactic Nuclei (AGN) is still unclear. The most common point of view is that there is a supermassive black hole in the centre of active galaxy with mass approximately $10^8 \div 10^9 M_{\odot}$ (Rees, 1984). Accretion on the black hole leads to the formation of powerful turbulent processes in accretion discs which effectively heat the plasma and generate magnetic field of the order of $10^4 G$. Ejection of plasma from discs with frozen magnetic field and emission lead to the formation of collimated streams which transfer energy to large distances, up to 10^5 pc. Besides, the processes of generation of electron–positron plasma may occur in the magnetospheres of the black holes as well as in the vicinity of accretion discs. Particles are created in collisions of high–energy photons produced by inverse Compton scattering of ultraviolet photons emitted from disk with fast particles accelerated by magnetic reconnection within disk or within magnetospheres of the rotating black hole, where equilibrium charge density changes its sign (see, for example Beskin, Istomin & Pariev, 1992b). Electron–positron plasma forms pinched streams (jets) which have radii of the order of one parsec. The energy density of electromagnetic field in these jets greatly exceeds the energy density of electrons and positrons taking into account their rest energy. Rotation of the black hole and the accretion disc is transmitted to the jet due to magnetic coupling, where strong radial electric field E_r arises. Drift in this field and in the longitudinal magnetic field B_z frozen into plasma leads to differential rotation. Electric current transferred by the jet produces azimuthal magnetic field B_ϕ , and magnetic field lines are twisted into spirals. Energy

* E-mail: beres@td.lpi.ac.ru † E-mail: istomin@td.lpi.ac.ru

²Steward Observatory, University of Arizona, 933 North Cherry Avenue, Tucson, AZ 85721, USA

2

in the jet is transferred by the Pointing vector which is proportional to the product of radial electric field and azimuthal magnetic field. Therefore, there is no problem of energy transfer along the jet on large distances as there is in the case when the main energy is in the hydrodynamic motion.

The most amazing facts of the jets from AGN are their high collimation (the ratio of the length to the diameter is a few orders of magnitude), stability and apparent superluminal velocities of distinct knots (Begelman, Blandford & Rees, 1984). The hydrodynamic and MHD stability of jets was investigated in many works (Blandford & Pringle, 1976; Torricelli-Ciamponi & Petrini, 1990; Appl, Camenzind, 1992). As to the stability of the electron-positron jets, rotating and moving with relativistic speed, it was shown in papers by Istomin & Pariev, 1994 and Istomin & Pariev, 1996 that they are stable with respect to axisymmetric as well as spiral perturbations. The physical reason for stability is the shear of the magnetic field, which in the case of small hydrodynamic pressure of plasma stabilizes small oscillations. Perturbations do not increase with time (Im $\omega \equiv 0$) or have small damping decrement (Im $\omega \approx 10^{-2} {\rm Re} \omega$) because of the resonance with Alfvén waves $\omega' = k'_{\parallel} c$. In electron–positron plasma, when the specific energy density and pressure are much less than the energy density of magnetic field, Alfvén velocity is equal to the speed of light in vacuum c (ω' and k' are the frequency and the wave vector in the plasma rest frame). Resonance condition is fulfilled on the specific magnetic surface and, in the case of cylindrical jet, at the definite distance from the axis. In the vicinity of that surface magnetic and electric fields of the wave reach large magnitudes. The particles of the jet are accelerated by the electric field here, which leads to the absorption of the energy of perturbation. Thus, the stability of the jet is connected directly with the production of energetic particles in the current. This resolves the problem of in situ acceleration of electrons and positrons producing synchrotron emission from knots observed along jets. In fact, as it is known (see Begelman at al., 1984), energetic particles accelerated in central region can not penetrate in the jet, they must loose their transverse momentum by synchrotron radiation already in the basement of the jet. Characteristic time of synchrotron losses is given by

$$\tau_s = \frac{3}{4} \frac{c\gamma_{\parallel}}{r_e \omega_{PO}^2}.$$

Here γ_{\parallel} is the longitudinal Lorentz–factor of the particle, $\gamma_{\parallel}=(1-v_{\parallel}^2/c^2)^{-1/2};\ r_e$ is the classical radius of the electron $r_e=e^2/mc^2;\ \omega_{B0}=eB/mc$ is the electron cyclotron frequency. Given $\gamma_{\parallel}=10,\ B=10^2G$ radiation time τ_s is approximately $3\cdot 10^5$ sec whereas the typical time of the flyby through the region of strong fields $\tau_f\approx\ell/c\approx 10^6$ sec. Here ℓ is the diameter of the jet, $\ell\approx 3\cdot 10^{16}$ cm.

In this paper we assume that the energy transferred along the jet, is mainly the electromagnetic energy which can be transmitted for long distances along the jets as along the wires. In this case it is very possible that part of that energy is in waves propagating along the jet, which are eigenmodes of cylindrical beam. The source of the wave motion is nonstationary processes in the magnetospheres of black hole and accretion disc. Short time variability on scales from days to months is actually observed in AGN (Mushotzky, Done & Pound, 1993; Witzel et al., 1993). Such a picture also gives a natural explanation of the superluminal motions but requires neither special orientation of the jet nor relativistic jet with high speed $(\beta = u/c > \sqrt{2}/2)$. As it was shown in papers by Istomin & Pariev, 1994 and Istomin & Pariev, 1996 there exist so called standing modes among eigenmodes in jets $(v_{group} \equiv 0)$ which are not propagate with finite velocity along jet but are only subject to diffuse spreading and, therefore, their amplitude is maximal. Phase velocity of these modes is greater than the speed of light. Crests of the wave move along the jet with superluminal velocity causing acceleration of the particles on the Alfvén surface. These regions can be the objects which are seen as bright knots with typical sizes of the order of the wavelength of the standing wave which is about the radius of the jet.

The purpose of our paper is the consideration of the acceleration processes near the Alfvén resonant surface, generation of the spectra of accelerated particles and calculation of the polarization of synchrotron radiation generated by these particles.

2 ACCELERATION OF PARTICLES

The equations of motion near the Alfvén surface are rather complicated. Nevertheless, we can use drift equations (Sivukhin, 1965) because the Larmor radius of relativistic electrons and positrons $r_c = \mathcal{E}/eB \approx 10^7 \, \mathrm{cm}$ (if we take $B \approx 10^{-3}$ and $\gamma \approx 10$) is much less then radius of the jet and the width of resonant surface r_0 (see expression (31*)).

$$\frac{d\mathbf{r}}{dt} = v_{\parallel} \frac{\mathbf{B}}{B} + \frac{c}{B^{2}} [\mathbf{E} \times \mathbf{B}] + \frac{\mathcal{E}v_{\parallel}^{2}}{ecB^{4}} [\mathbf{B} \times (\mathbf{B}\nabla)\mathbf{B}] + \frac{\mathcal{E}v_{\perp}^{2}}{2ecB^{3}} [\mathbf{B} \times \nabla B];$$

$$\frac{d\mathcal{E}}{dt} = e\mathbf{E} \frac{d\mathbf{r}}{dt} + \frac{\mathcal{E}v_{\perp}^{2}}{2c^{2}B} \frac{\partial B}{\partial t};$$

$$\frac{dJ_{\perp}}{dt} = 0.$$
(1)

Here the electric field is assumed to be small compared with the magnetic one, \mathcal{E} is the energy of the particle, $J_{\perp} = p_{\perp}^2/B$. Electromagnetic fields are equal to the sum of stationary fields (without subscript) and wave fields (subscript 1). For cylindrical

jet the stationary configuration of fields is (Istomin & Pariev, 1994) (c=1):

$$\mathbf{B} = B_z \mathbf{e}_z + B_\phi \mathbf{e}_\phi; \quad B_\phi = \Omega^F r B_z;$$

$$\mathbf{u} = K \mathbf{B} + \Omega^F r \mathbf{e}_\phi;$$

$$\mathbf{E} = -\Omega^F r [\mathbf{e}_\phi \times \mathbf{B}],$$
(2)

where r, ϕ, z are cylindrical coordinates. In components

$$\mathbf{B} = (0, \Omega^F r, 1) B_z,$$

$$\mathbf{E} = (-\Omega^F r, 0, 0) B_z.$$

Here Ω^F and K are functions of r, B_z does not depend on r. Stationary electric field, which has an absolute value of $\Omega^F r B_z$, is not small compared to the magnetic field when $\Omega^F r > 1$, therefore we must consider our equations in the frame moving with plasma where $E \equiv 0$. There are a lot of such reference frames because there is an arbitrary parameter K(r) in the expression for the velocity of plasma which determines the radial profile of longitudinal velocity. $K(r)B_z$ is the velocity along the magnetic field which is not related to the rotation. We choose, however, the velocity \mathbf{u} which minimizes the kinetic energy of the plasma in the stationary reference frame.

$$\mathbf{u} = \frac{(0, \Omega^F r, -(\Omega^F r)^2)}{1 + (\Omega^F r)^2}.$$
(3)

It seems that the plasma moves with that velocity in real jets. Fields in the wave calculated in terms of Lagrangian displacement ξ are equal (here we drop out the phase coefficient $\exp(-i\omega t + ikz + im\phi)$)

$$B_{r1} = iB_z F \xi;$$

$$B_{\phi 1} = -B_z (\Omega^F r \frac{d\xi}{dr} + \xi \frac{d}{dr} (\Omega^F r) + \frac{k}{S} D);$$

$$B_{z1} = B_z (-\frac{d\xi}{dr} - \frac{\xi}{r} + \frac{m}{rS} D);$$

$$E_{r1} = B_z (\Omega^F r \frac{d\xi}{dr} + \xi \frac{d}{dr} (\Omega^F r) - \frac{\omega}{S} D);$$

$$E_{\phi 1} = -iB_z (\omega - m\Omega^F) \xi;$$

$$E_{z1} = iB_z \Omega^F r (\omega + k) \xi;$$

$$(4)$$

where

$$D = r \frac{d\xi}{dr} \left(\Omega^F(\omega + k) - \frac{m}{r^2} \right) - \xi \left(\Omega^F(\omega + k) + \frac{m}{r^2} \right),$$
$$F = k + m\Omega^F,$$
$$S = \omega^2 - k^2 - m^2/r^2.$$

For Lagrangian displacement ξ and dimensionless pressure disturbance $p_* = 4\pi P_1/B_z^2$ we have a system of differential equations obtained by Istomin & Pariev, 1996:

$$\begin{cases}
A \frac{1}{r} \frac{d}{dr} (r\xi) &= C_1 \xi - C_2 p_*; \\
A \frac{dp_*}{dr} &= C_3 \xi - C_1 p_*.
\end{cases} (5)$$

Here

$$C_{1} = \frac{2}{r} \left(m\Omega^{F} - (\Omega^{F}r)^{2}(\omega + k) \right);$$

$$C_{2} = -\frac{\omega^{2} - k^{2} - m^{2}/r^{2}}{\omega + k};$$

$$C_{3} = -(\omega + k)(A^{2} - 4\Omega^{F^{2}});$$

$$A = k - \omega + 2m\Omega^{F} - (\Omega^{F}r)^{2}(\omega + k).$$

Let us expand equations (5) near the Alfvén surface, i.e. near the point r_A where $A(r_A) = 0$. Denoting $x = r - r_A$ we get

$$\begin{cases} \frac{d\xi_r}{dx} = \frac{1}{A'x} (C_1\xi_r - C_2p_*); \\ \frac{dp_*}{dx} = \frac{1}{A'x} (C_3\xi_r - C_1p_*), \end{cases}$$
 (6)

where $A' = \frac{dA}{dr}\Big|_{r=r_A}$. The general solution of these equations is

$$\begin{pmatrix} \xi \\ p_* \end{pmatrix} = \alpha_1 \begin{pmatrix} C_2 \ln x \\ C_1 \ln x - A' \end{pmatrix} + \alpha_2 \begin{pmatrix} C_2 \\ C_1 \end{pmatrix} \tag{7}$$

where α_1 and α_2 are constants. They are not arbitrary, rather they are fixed by the boundary conditions on ξ and p_* obtained from solving general equation (5). We see that ξ and p_* have a logarithmic singularity at the Alfvén point. Later we adhere to our expansion over $r - r_A$, assuming $r = r_A$, A = 0 whenever the quantities under consideration have no singularities at $r = r_A$. Let us calculate $d\mathbf{r}/dt$ and $d\mathcal{E}/dt$ in the first order by fields of the wave. Remembering that $\mathbf{E} = \mathbf{0}$ in our reference frame and knowing that terms with the energy \mathcal{E} contain small parameter which is the ratio of the Larmour radius to the jet radius or to the characteristic length of variations of zero order fields we can simplify drift equations as follows,

$$\left(\frac{d\mathbf{r}}{dt}\right)_0 = v_{\parallel}\mathbf{e}_z,$$

$$\left(\frac{d\mathbf{r}}{dt}\right)_{1} = v_{\parallel} \frac{\mathbf{B}_{1}}{B} - v_{\parallel} \frac{\mathbf{B}(\mathbf{B} \cdot \mathbf{B}_{1})}{B^{3}} + \frac{[\mathbf{E}_{1} \times \mathbf{B}]}{B^{2}}$$

$$\tag{8}$$

Here subscript 0 denotes the zero order term and 1 denotes the first order term. The force of inertia is also present in the expression of $d\mathbf{r}/dt$ (see Sivukhin, 1965), but the term with inertia force contains the mass, has the same order as terms with energy and is omitted consequently. For $d\mathcal{E}/dt$ we will also not take into account the inertia force because it is smaller than gradient terms such as $\mathcal{E}v_{\parallel}^2[\mathbf{B}\times(\mathbf{B}\nabla)\mathbf{B}]/ecB^4$. When we substitute \mathbf{B}_1 and \mathbf{E}_1 into (8) we get

$$\left(\frac{dr}{dt}\right)_1 = (v_{\parallel} - 1)\frac{i\xi F}{\gamma},\tag{8*}$$

where $\gamma = \sqrt{1 + (\Omega^F r)^2}$ is the Lorentz factor corresponding to the velocity of the moving frame. ξ depends on z, ϕ, t by $\exp\{-i\omega t + ikz + im\phi\}$. The phase of the wave Ψ which is "seen" by the particle can be calculated using Lorentz transformation formulae $\Psi = -\frac{F}{\gamma}t' + \frac{F}{\gamma}z'$. Assuming $dz/dt = v_{\parallel}$ we get $\Psi = (v_{\parallel} - 1)\frac{F}{\gamma}t'$. As we see the coefficient for the phase coincides with the coefficient in (8*). It confirms our calculations because ξ is the Lagrangian displacement. The question of the trajectory of the particle will be considered later.

Now we proceed with calculating $d\mathcal{E}/dt$.

$$\frac{d\mathcal{E}}{dt} = e\mathbf{E}_1 \cdot \left(\frac{d\mathbf{r}}{dt}\right)_0 + \frac{\mathcal{E}v_\perp}{2B} \frac{\partial B_1}{\partial t}.$$
 (9)

After substitution of expressions for fields into (9) we get

$$\frac{d\mathcal{E}}{dt} = \mathcal{E}v_{\perp}^{2} \left(-\frac{iF}{\gamma} \right) \frac{\xi}{rS} (\omega + k) [F - \omega], \tag{10}$$

or, combining with (8*)

$$\frac{d\mathcal{E}}{dr} = \frac{\mathcal{E}v_{\perp}^2}{1 - v_{\parallel}} \left(\frac{(\omega + k)[F - \omega]}{rS} \right). \tag{11}$$

As we see, \mathcal{E} is proportional to the r if we do not take into account dependence of the right hand side on \mathcal{E} Therefore it makes sense to consider motion of the particle "smoothed" over many periods. Taking the r-component of (8*), we have

$$\frac{dx}{dt} = i\omega^* \xi(x) e^{i\omega^* t}, \quad \omega^* = (v_{\parallel} - 1) \frac{F}{\gamma}. \tag{12}$$

Near the Alfvén resonance $\xi(x)$ has a logarithmic singularity

$$\frac{dx}{dt} = \omega^* [A \ln x \sin(\omega^* t) + B \cos(\omega^* t)]. \tag{13}$$

It is clear that ω^*A and ω^*B are dimensionless amplitudes of the perturbation (remember, that c=1). Let us average equation (13) expanding it in small amplitude of oscillation of a particle in the field of the wave. We denote perturbations of the zero, first, second orders as x_0 , x_1 , x_2 .

$$\frac{dx_1}{dt} = \omega^* [A \ln x_0 \sin(\omega^* t) + B \cos(\omega^* t)]$$

$$x_1 = -A \ln x_0 \cos(\omega^* t) + B \sin(\omega^* t)$$

$$\frac{dx_2}{dt} = \omega^* [A \ln |x_0 - A \ln x_0 \cos(\omega^* t) + B \sin(\omega^* t) | \sin(\omega^* t) + B \cos(\omega^* t)]$$

$$\frac{\overline{dx_2}}{dt} = \omega^* AB \frac{1}{2x_0}$$

Now let us replace x_0 and x_2 by x. We obtain smoothed equation of motion

$$\frac{d\bar{x}}{dt} = \omega^* \frac{AB}{2x},$$

which has the solution

$$\bar{x} = \sqrt{\omega^* A B t}.\tag{14}$$

From equations (11), (14) it follows that the particle gains energy drifting along the r axis. However, its acceleration rate is proportional to the transverse momentum which remains constant in accordance with the drift equations (1)

$$\frac{dp_{\perp}}{dt} \propto \frac{dJ_{\perp}}{dt} = 0.$$

Here we do not take into account the change of the magnetic field connected with the wave field because of $B_1 \ll B$. However, because of synchrotron losses J_{\perp} and p_{\perp} are monotonically decreased according to $(\omega_B = \omega_{B0} \frac{m_0 c^2}{\mathcal{E}})$

$$\frac{dJ_{\perp}}{dt} = -\frac{4}{3}\omega_B^2 \frac{r_e}{c} \left(\frac{\mathcal{E}}{m_0 c^2}\right)^3 \left(1 - \frac{v_{\parallel}^2}{c^2}\right) J_{\perp},\tag{15}$$

this leads to the situation when $p_{\parallel} > p_{\perp}$. Such anisotropic distribution can become unstable to the excitation of electromagnetic waves which results in isotropization of distribution function in the momentum space. We will treat instability of plasma according to Mikhaylovskii, 1968. Mikhaylovskii, 1968 showed that in the case $p_{\parallel} > p_{\perp}$ only perturbations with $\kappa_z = 0$ must be taken into account. The frequencies of these perturbations with $\kappa \perp \mathbf{B}$ are the solutions of dispersion relation $\varepsilon_{33} - N^2 = 0$, where ε_{33} is the component of dielectric tensor along the magnetic field, $N = c\kappa/\omega$. The contribution of i sort of plasma into ε_{33} is given by the general formula

$$\varepsilon_{33}^{(i)} = \frac{4\pi e^2}{\omega} \left\langle \sum_{n=-\infty}^{\infty} \frac{v_z J_n^2 \left(\kappa v_{\perp} / \omega_B\right)}{\omega - n\omega_B} \left[\frac{\partial F}{\partial p_z} - \frac{n\omega_B}{\omega} \left(\frac{\partial F}{\partial p_z} - \frac{v_z}{v_{\perp}} \frac{\partial F}{\partial p_{\perp}} \right) \right] \right\rangle$$
(16)

Here $\langle \dots \rangle$ means $\int \dots p_{\perp} dp_{\perp} dp_z$ and the distribution function F is chosen so that $\int F p_{\perp} dp_{\perp} dp_z = n_0$, n_0 is the equilibrium particle density. From formula (16) it is seen that electron and positrons make an equal contribution to the ε_{33} because the sum is symmetric to the simultaneous replacement of n with -n and of e with -e. After some calculations we get

$$\varepsilon_{33} - 1 = \frac{4\pi e^2}{\omega^2} \left\langle v_z \left[\frac{\partial F}{\partial p_z} - \left(1 - J_0^2 \left(\frac{\kappa v_\perp}{\omega_B} \right) \right) \frac{v_z}{v_\perp} \frac{\partial F}{\partial p_\perp} \right] \right\rangle + 2\omega^2 \left\langle \sum_{n=1}^{\infty} \frac{\frac{v_z^2}{v_\perp} \frac{\partial F}{\partial p_\perp}}{\omega^2 - n^2 \omega_B^2} J_n^2 \left(\frac{\kappa v_\perp}{\omega_B} \right) \right\rangle. \tag{17}$$

Dispersion relation of the small oscillations has the form

$$\frac{c^2 \kappa^2}{4\pi e^2} = \frac{\omega^2}{4\pi e^2} + \left\langle v_z \left[\frac{\partial F}{\partial p_z} - \left(1 - J_0^2 \right) \frac{v_z}{v_\perp} \frac{\partial F}{\partial p_\perp} \right] + 2\omega^2 \sum_{n=1}^{\infty} \frac{\frac{v_z^2}{v_\perp} \frac{\partial F}{\partial p_\perp}}{\omega^2 - n^2 \omega_B^2} J_n^2 \right\rangle.$$
(18)

Study of (18) shows (Mikhaylovskii, 1968) that instability arises at small values of ω . Therefore let us assume ω to be small and find it

$$\omega^{2} = \frac{\frac{c^{2}\kappa^{2}}{4\pi e^{2}} - \left\langle v_{z} \frac{\partial F}{\partial p_{z}} \right\rangle + \left\langle \left(1 - J_{0}^{2}\right) \frac{v_{z}^{2}}{v_{\perp}} \frac{\partial F}{\partial p_{\perp}} \right\rangle}{\frac{1}{4\pi e^{2}} - 2 \sum_{n=1}^{\infty} \left\langle \frac{v_{z}^{2}}{v_{\perp}} \frac{\partial F}{\partial p_{\perp}} J_{n}^{2} / n^{2} \omega_{B}^{2} \right\rangle}.$$
(19)

For further calculations we assume that κv_{\perp} is of the order of ω_B and estimate expression (19) taking into account only first terms of expansion of Bessel function over its arguments.

$$\omega^{2} = \frac{c^{2}\kappa^{2} - 4\pi e^{2} \left\langle v_{z} \frac{\partial F}{\partial p_{z}} - \frac{1}{2} \left(\frac{\kappa}{\omega_{B}} \right)^{2} v_{z}^{2} v_{\perp} \frac{\partial F}{\partial p_{\perp}} \right\rangle}{1 - 4\pi e^{2} \left\langle \frac{1}{2\omega_{B}^{2}} \left(\frac{\kappa}{\omega_{B}} \right)^{2} v_{z}^{2} v_{\perp} \frac{\partial F}{\partial p_{\perp}} \right\rangle}.$$
 (20)

Let us take integrals in (20) in parts remembering that $\omega_B \propto 1/\gamma$. Here $\gamma = \mathcal{E}/m_0c^2$. As was shown in (Mikhaylovskii, 1968) the maximum increment is achieved at the values of $\kappa^2 \simeq \langle \omega_B^2/v_\perp^2 \rangle$. We will see later that instability at this κ satisfies our requirements

$$\omega^{2} = \omega_{B0}^{2} \frac{m_{0}^{2} c^{2} \frac{\omega_{B0}^{2}}{\omega_{p}^{2}} + \left\langle p_{\perp}^{2} \right\rangle \left\langle \frac{1}{\gamma^{3}} \right\rangle + \left\langle p_{\perp}^{2} \right\rangle \left\langle \frac{p_{\perp}^{2}}{\gamma^{3} m_{0}^{2} c^{2}} \right\rangle - \frac{1}{2} \left(\left\langle \frac{p_{z}^{2}}{\gamma^{3}} \right\rangle + \left\langle \frac{p_{z}^{4}}{\gamma^{3} m_{0}^{2} c^{4}} \right\rangle + \left\langle \frac{p_{z}^{2}}{\gamma} \right\rangle \right)}{\frac{\omega_{B0}^{2}}{\omega_{p}^{2}} \left\langle p_{\perp}^{2} \right\rangle + \left\langle p_{z}^{2} \gamma \right\rangle + \frac{1}{2} \left\langle \frac{p_{z}^{2} p_{\perp}^{2}}{\gamma m_{0}^{2} c^{2}} \right\rangle}.$$
(21)

Here $\omega_p^2 = 4\pi ne^2/m$ is the plasma frequency squared. We continue our consideration by simplifying our assumption about the distribution function. Let all particles have equal p_{\perp} and p_{\parallel} . This is rather rough approximation but it allows us to understand

where the instability threshold is. So, remove all signs <> and for the sake of simplicity let $m_0=c=1$.

$$\omega^2 \approx \frac{\omega_{B0}^2}{\gamma^2} \frac{\gamma^4/\beta + p_\perp^2 + p_\perp^4 - (p_z^2 + p_z^4 + \gamma^2 p_z^2)/2}{\gamma^2/\beta + \gamma^2 p_z^2 + p_z^2 p_\perp^2/2},$$
(22)

where $\beta = 4\pi nmc^2 \gamma/B^2$ is the ratio of the particle pressure to the magnetic field pressure. Although β depends on energy let it to be constant to know where the threshold of the resonance is in the case of fixed energy. If we consider ultrarelativistic particles $p^2 \ll p^4$, we will have for the ratio of p_z to p_\perp at which the imaginary part of ω arises

$$\frac{p_z^2}{p_\perp^2} = \frac{4 - \beta + \sqrt{\beta(17\beta - 8)}}{4(\beta - 1)}. (23)$$

We denote the threshold of stability $p_z/p_\perp = \alpha$, $\alpha > 1$ (Expression (23) is not quite valid for very large $\beta > 8$ but we do not consider large β here). Im ω arises when $p_z > \alpha p_\perp$. As we see from (22) instability is fast because the increment of it is proportional to the cyclotron frequency. In our case it is the least typical time and it is less then the wave period by twelve orders of magnitude. Because of this fact we will always assume the distribution function to be such that $\text{Im}\omega = 0$. More concrete, we will consider $p_z/p_\perp = \alpha = \text{const.}$ Assuming constant pitch angle for all particles may be confusing because as a result of the synchrotron emission of these particles we will obtain sharp maximum of the emission in directions close to this angle. But one has to remember that the emission must be integrated in the different parts of the jet, and always there will be particles found having velocities pointed to a given point in the sky, since in different parts of the jet we transit into a different reference frames. Thus the final result may be less rough than the intermediate. Now we understand that $dJ_\perp/dt \neq 0$ because of the anisotropic plasma instability and instead of the equation $dJ_\perp = \text{constant}$ we use $p_z/p_\perp = \alpha = \text{constant}$. For the derivative of energy we write equation (11) adding the synchrotron losses.

$$\frac{d\mathcal{E}}{dt} = \frac{\mathcal{E}v_{\perp}^2}{1 - v_{\parallel}} \frac{(\omega + k)[F - \omega]}{rS} v_x - \frac{2}{3} \frac{p_{\perp}^2}{m_0} \omega_{B0}^2 r_e. \tag{24}$$

Substituting v_x from (14) we obtain

$$\frac{d\mathcal{E}}{dt} = \frac{\mathcal{E}}{1 + \alpha^2 - \alpha\sqrt{1 + \alpha^2}} \frac{(\omega + k)[F - \omega]}{rS} \left(\frac{\omega^* AB}{4t}\right)^{1/2} - \frac{2}{3} \frac{\mathcal{E}^2}{1 + \alpha^2} \omega_{B0}^2 \frac{r_e}{m_0}.$$
 (25)

Let us introduce some conventional signs

$$Q = \frac{1}{1 + \alpha^2 - \alpha\sqrt{1 + \alpha^2}} \frac{(\omega + k)[F - \omega]}{S};$$

$$\mathcal{E}_{1} = \frac{3}{4} \frac{m_{0}}{1 + 2\alpha^{2} - 2\alpha\sqrt{1 + \alpha^{2}}} \left(\frac{(\omega + k)[F - \omega]}{S}\right)^{2} \frac{\omega^{*2}AB}{\omega_{B0}^{2} r_{e} r^{2} \omega^{*}}.$$
 (26)

Here $(\omega + k)[F - \omega]/S$ is the fixed number for a given values of wavenumbers of the perturbation m and k. It is large near the fast magnetosonic resonance surface S = 0. The coefficient of $1/(\omega_{B0}^2 r_e r^2 \omega^*)$ is a large number. In the case of an AGN jet $B \approx 10^{-2}$ G (Begelman at al., 1984), $r \approx 1$ pc it equals approximately to the 10^4 . The value of $\omega^{*2}AB$ as we noted after formula (13) is the dimensionless amplitude of perturbation squared. Now taking into account our notations the solution for \mathcal{E} has the form

$$\mathcal{E} = \left(\frac{1}{\mathcal{E}_1} \left(Q \frac{x}{r} - 1 \right) + \left(\frac{1}{\mathcal{E}_1} + \frac{1}{\mathcal{E}_0} \right) \exp\left\{ -Q \frac{x}{r} \right\} \right)^{-1}.$$
 (27)

Here $\mathcal{E}_0 = \mathcal{E}(x=0)$. Let us denote Qx/r = x'. We assume that x' can be large because of the quantity Q is large. It is seen that first \mathcal{E} exponentially increases and then decreases as 1/x'. We consider an asymptotic behaviour of \mathcal{E} in the case of different x' and \mathcal{E}_0 . In the case of $\mathcal{E}_0 < \mathcal{E}_1$

$$\mathcal{E} = \begin{cases} \mathcal{E}_1/x', & x'e^{x'} > \mathcal{E}_1/\mathcal{E}_0 \\ \mathcal{E}_0e^{x'}, & x'e^{x'} < \mathcal{E}_1/\mathcal{E}_0 \end{cases}$$
(27*)

In the case of $\mathcal{E}_0 > \mathcal{E}_1$

$$\mathcal{E} = \left\{ \begin{array}{ll} \mathcal{E}_1/x', & x' > 1 \\ 2\mathcal{E}_1/{x'}^2, & x' < 1 \end{array} \right.$$

We reject the case when $\mathcal{E}_0 > \mathcal{E}_1$ assuming that the typical initial energy is much less then \mathcal{E}_1 .

3 FORMATION OF THE SPECTRUM OF ACCELERATED PARTICLES

Our goal is to calculate the distribution function averaged over x' knowing the distribution function at x = 0. We will consider the stationary case, when $\partial f/\partial t = 0$. Let the distribution function to be given at the point x'_0 as a function of $\mathcal{E}' = \mathcal{E}/\mathcal{E}_1$. Then the number of particles

$$dN = f(\mathcal{E}_0', x_0') d\mathcal{E}_0' dx_0' = f\left(\mathcal{E}_0'(\mathcal{E}', x'), x_0'(\mathcal{E}', x')\right) \frac{D(\mathcal{E}_0', x_0')}{D(\mathcal{E}', x')} d\mathcal{E}' dx'.$$

Further we omit primes. Thus if we know the trajectory $\mathcal{E}_0(\mathcal{E}, x), x_0(\mathcal{E}, x)$ we may obtain the distribution function at the point \mathcal{E}, x . In our case the Jacobian $D(\mathcal{E}'_0, x'_0)/D(\mathcal{E}', x')$ is not equal to unity because variables \mathcal{E}, x are not canonical. So,

$$F(\mathcal{E}, x) = f\left(\mathcal{E}_0(\mathcal{E}, x), x_0(\mathcal{E}, x)\right) \frac{D(\mathcal{E}_0, x_0)}{D(\mathcal{E}, x)}.$$
(29)

The formula analogous to the (27) but with the arbitrary reference point x_0 is the following

$$\mathcal{E} = \left\{ x - 1 + (1/\mathcal{E}(x_0) - x_0 + 1) \exp(-x + x_0) \right\}^{-1} \tag{30}$$

Substituting \mathcal{E}_0 expressed from (30) into (29) we obtain

$$F(\mathcal{E}, x) = f\left(\left\{-1 + x_0 + \left(\frac{1}{\mathcal{E}} - x + 1\right) \exp(x - x_0)\right\}^{-1}, x_0\right) \left(\frac{\partial \mathcal{E}_0}{\partial \mathcal{E}} \frac{\partial x_0}{\partial x} - \frac{\partial \mathcal{E}_0}{\partial x} \frac{\partial x_0}{\partial \mathcal{E}}\right) =$$
(31)

$$f\left(\left\{-1+x_0+\left(\frac{1}{\mathcal{E}}-x+1\right)\exp(x-x_0)\right\}^{-1},x_0\right)\frac{\mathcal{E}_0^2}{\mathcal{E}^2}\exp(x-x_0)\frac{x}{x_0}$$

We know that initial fast particles are born near the point x=0, therefore in the last formula we let $x_0=0$ everywhere except x_0 in the denominator. Physically $f(\mathcal{E}_0,0)$ is the particle density at zero point and x_0 is the distance at which our formulae, for instance (14), do not work. Because of the small imaginary part of ω which is an attenuation increment of the wave (Istomin & Pariev, 1996) the divergence $\ln x$ at the resonance is cut at the point

$$r_0 \approx \left| \frac{A(r = r_A)}{dA/dr(r = r_A)} \right|.$$
 (31*)

Here $A(r = r_A)$ is not equal to zero as we assumed in the previous text, but determined by the small value of the imaginary part of ω . Thus, x_0 is the width of the resonance $x_0 = Qr_0/r_A$. Eventually,

$$F(\mathcal{E}, x) = f_0 \left(\left\{ -1 + \left(\frac{1}{\mathcal{E}} - x + 1 \right) \exp(x) \right\}^{-1} \right) \frac{\mathcal{E}_0^2}{\mathcal{E}^2} \exp(x) \frac{x}{x_0}$$
 (32)

Because the width of the resonance r_0 and the width of the acceleration region Δr , which is some function of r_0 , are small compared with the jet radius we average the distribution function over the jet radius near the resonance surface

$$\bar{f}(\mathcal{E}) = \frac{1}{\Delta x} \int_{0}^{\infty} F(\mathcal{E}, x) dx, \quad \Delta x = \frac{Q}{r_A} \Delta r.$$
 (34)

Denoting $N(\mathcal{E}) = \bar{f}(\mathcal{E})\Delta x$ we obtain

$$\bar{N}(\mathcal{E}) = \int_{0}^{\infty} f_0 \left(\left\{ -1 + \left(\frac{1}{\mathcal{E}} - x + 1 \right) \exp(x) \right\}^{-1} \right) \frac{\mathcal{E}_0^2}{\mathcal{E}^2} \exp(x) \frac{x}{x_0} dx. \tag{35}$$

Let us change variable of integration to \mathcal{E}_0 . The dependence of \mathcal{E}_0 versus x under fixed \mathcal{E} is presented in Fig. 1.

The value of \mathcal{E}_{min} is

$$\mathcal{E}_{min} = 1/(-1 + exp(1/\mathcal{E})). \tag{36*}$$

Because the function $x = x(\mathcal{E}_0)$ has two branches the equation (35) is transformed into

$$N(\mathcal{E}) = \frac{1}{\mathcal{E}^2 x_0} \int_{\mathcal{E}_{min}}^{\mathcal{E}} f_0(\mathcal{E}_0) \frac{x}{1/\mathcal{E} - x} d\mathcal{E}_0 +$$

$$\frac{1}{\mathcal{E}^2 x_0} \int_{\mathcal{E}_{min}}^{\infty} f_0(\mathcal{E}_0) \frac{x}{1/\mathcal{E} - x} d\mathcal{E}_0, \tag{36}$$

where in the first integral x is taken on the first branch of $x(\mathcal{E}_0)$ and in the second integral on the second branch. Let us make some natural assumptions. Initial distribution function is cut off at the typical energy of T_0 , provided that $T_0 \ll 1$ (bearing in mind that T_0 as well as \mathcal{E} are in the units of energy \mathcal{E}_1 (26)). Let us calculate $N(\mathcal{E})$ in the region, where $T_0 \ll \mathcal{E} \ll 1$, because it is seen from equations (36) and (36*) that in the case $\mathcal{E} \sim 1$ the integral is small. Let us evaluate the contribution of the singularity $x = 1/\mathcal{E}$ in integrals (36)

$$\mathcal{E}_0 - \mathcal{E}_{min} = \frac{d^2 \mathcal{E}_0}{dx^2} \left(x - \frac{1}{\mathcal{E}} \right)^2$$

Figure 1. The dependence of \mathcal{E}_0 versus x (the energy \mathcal{E} and the distance x are in the values of \mathcal{E}_1 and r/Q (26) correspondently)

Integral near the singularity is

$$\frac{1}{\mathcal{E}^2} \int_{\mathcal{E}} f_0(\mathcal{E}_{min}) \frac{\frac{1}{\mathcal{E}} \sqrt{\frac{d^2 \mathcal{E}_0}{dx^2}}}{x_0 \sqrt{\mathcal{E}_0 - \mathcal{E}_{min}}} d\mathcal{E}_0 \sim \sqrt{\mathcal{E}_0 - \mathcal{E}_{min}}.$$

Thus, its contribution is small. Because the main contribution to expression (30) is when x is far from $1/\mathcal{E}$, we may use asymptotic values of x (see equation (27*)): $x \approx \ln(\mathcal{E}/\mathcal{E}_0)$ on the first branch; $x \approx 1/\mathcal{E} + 1$ on the second branch and obtain that

$$N(\mathcal{E}) = \frac{1}{\mathcal{E}^2 x_0} \int_{\mathcal{E}_{min}}^{\mathcal{E}} f_0(\mathcal{E}_0) \frac{\ln(\mathcal{E}/\mathcal{E}_0)}{1/\mathcal{E} - \ln(\mathcal{E}_0/\mathcal{E})} d\mathcal{E}_0 + \frac{1}{\mathcal{E}^2 x_0} \int_{\mathcal{E}_{min}}^{\infty} f_0(\mathcal{E}_0) \frac{1}{\mathcal{E}} d\mathcal{E}_0.$$
 (37)

Let us consider only $\mathcal{E}_{min} \ll T_0$ i.e. $\mathcal{E} \ll -1/\ln T_0$ because in the reverse case the integral is small. Now we can replace \mathcal{E}_{min} by 0 and also $1/\mathcal{E} \gg \ln(\mathcal{E}/\mathcal{E}_0)$. Equation (37) becomes

$$N(\mathcal{E}) = \frac{1}{\mathcal{E}x_0} \int_0^{\mathcal{E}} f_0(\mathcal{E}_0)(-\ln \mathcal{E}_0) d\mathcal{E}_0 + \frac{n}{\mathcal{E}^3 x_0},$$
(38)

where $n = \int_0^\infty f_0(\mathcal{E}_0) d\mathcal{E}_0$. Rewriting expression (38) as

$$N(\mathcal{E}) = \frac{n}{\mathcal{E}x_0} < -\ln \mathcal{E}_0 > + \frac{n}{\mathcal{E}^3 x_0}$$
(39)

we note that the first term is approximately equal to

$$\frac{n}{\mathcal{E}x_0}(-\ln T_0)$$

and is small compared to the second term because non-equality $1/\mathcal{E}^2 \gg -\ln T_0$ is the consequence of non-equality $1/\mathcal{E} \gg -\ln T_0$. Therefore $N(\mathcal{E}) \propto 1/\mathcal{E}^3$ and we obtain power law distribution with the index -3. The validity region of this formula $T_0 < \mathcal{E} < -1/\ln T_0$ is quite large.

We performed integration in equation (36) numerically having taken Gaussian initial distribution with different temperatures. Results are presented in Figs. 2 and 3.

The value of power law index is minus three for small energies and rises slightly before the cut off of the distribution function. However, the value -3 of power law index is not applicable all the way down to $\mathcal{E} = 0$. The natural boundary is the width of the acceleration region Δr (see expression (31*)). Because the main contribution to the integral (31*) is from the region near the point $x = 1/\mathcal{E} + 1$ the lower limit for power law $1/\mathcal{E}^3$ is $\mathcal{E}_l = 1/\Delta x$. We also found mean power law index for the distribution of particles between energies \mathcal{E}_l and $-1/\ln T_0$. Results are presented in Fig. 4.

One remaining question in the formation of the spectrum of energetic particles is the origin of the initial particles, since in the first order on perturbed fields there is no acceleration of the cold plasma in equations (1). We have already mentioned that

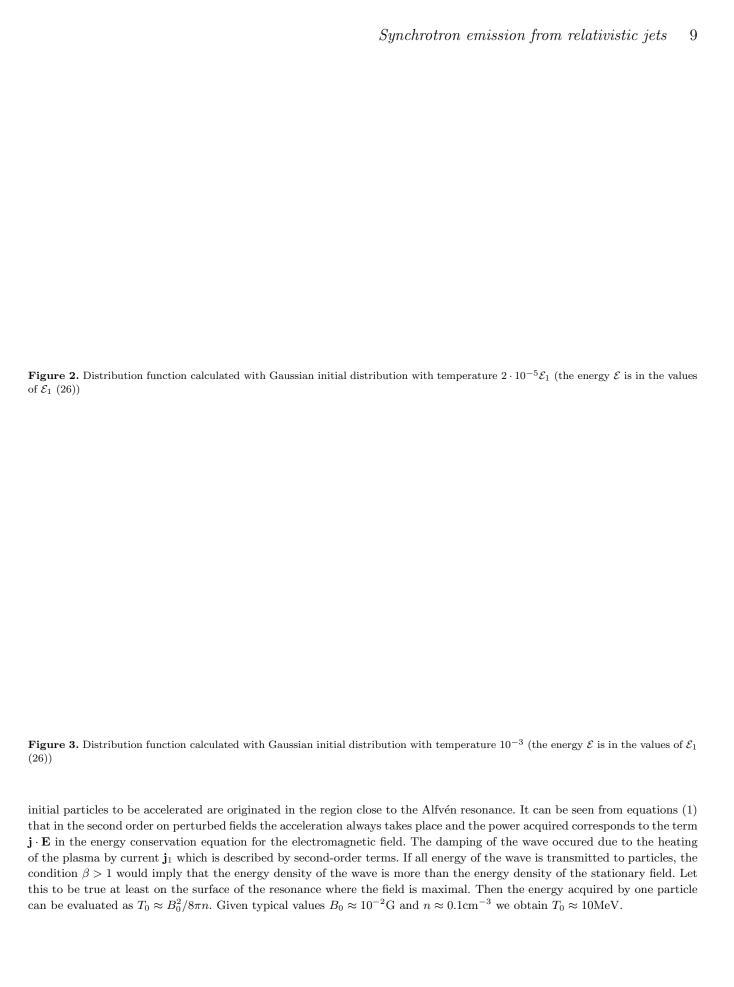


Figure 4. Averaged power law index (the initial particles energy T_0 is in the values of \mathcal{E}_1 (26))

4 SYNCHROTRON EMISSION.

Let us now consider synchrotron emission of accelerated particles in a cylindrical jet with spiral magnetic field. Consistently with the results of section 3 we take isotropic distribution function of emitting particle in momentum and power law in energy

$$dn = K_e \mathcal{E}^{-\gamma} d\mathcal{E} dV d\Omega_{\mathbf{p}} \tag{40}$$

Here dn is the number of particles in the energy interval $\mathcal{E}, \mathcal{E} + d\mathcal{E}, dV$ is elementary volume, $d\Omega_{\mathbf{p}}$ is the elementary solid angle in the direction of the particle momentum $\mathbf{p}, K_e = \text{constant}, \gamma = \text{constant}$. We will assume that ultralelativistic particles are distributed according (40) in the frame moving with plasma with the velocity

$$\mathbf{u}(r) = K\mathbf{B} + \Omega^F(r)r\mathbf{e}_{\phi}$$

We will consider two cases for the spatial distribution of particles, namely, uniform in the jet volume and concentrated close to the Alfvén resonant surface $r = r_A$. Influence of plasma on the emission of relativistic e^- and e^+ is neglected. Absorption and reabsorption are also not taken into account. At first we assume that there is no Doppler boosting i.e. $\mathbf{u} = 0$. In this case, according to e.g. Ginzburg, 1989, Stocks parameters are

$$I = \frac{\gamma + 7/3}{\gamma + 1} k(\nu) \int (B \sin \chi)^{1/2(\gamma + 1)} dR,$$

$$Q = k(\nu) \int (B \sin \chi)^{1/2(\gamma + 1)} \cos 2\tilde{\chi} dR,$$

$$U = k(\nu) \int (B \sin \chi)^{1/2(\gamma + 1)} \sin 2\tilde{\chi} dR,$$

$$V = 0,$$

$$(41)$$

Here integration is to be fulfilled along the line of sight in the region filled with particles,

$$k(\nu) = \frac{\sqrt{3}}{4} \Gamma\left(\frac{3\gamma-1}{12}\right) \Gamma\left(\frac{3\gamma+7}{12}\right) \frac{e^3}{mc^2} \left[\frac{3e}{2\pi m^3 c^5}\right]^{1/2(\gamma-1)} \nu^{-1/2(\gamma-1)} \frac{K_e}{D^2},$$

 χ is the angle between the magnetic field **B** and the line of sight, $\tilde{\chi}$ is the position angle in the picture plane of the electric field vector, D is the distance between the source and the observer. We will measure $\tilde{\chi}$ clockwise from the direction parallel to the jet axis. For ultrarelativistic particles V=0, and the emission has only linear polarization. Degree of polarization of the outgoing radiation is expressed as $\Pi=\sqrt{Q^2+U^2}/I$, resultant position angle of the electric field is found from

$$\cos 2\tilde{\chi}_{res} = \frac{Q}{\sqrt{Q^2 + U^2}}, \quad \sin 2\tilde{\chi}_{res} = \frac{U}{\sqrt{Q^2 + U^2}}, \quad 0 \le \tilde{\chi}_{res} < \pi.$$

Let h be the distance from the line of sight to the jet axis. We will assume that h is signed, i.e changing from -R to R for the different lines of sight. We will denote the angle between the jet axis and the direction to the observer as θ . In cylindrical

coordinates

$$I = \frac{\gamma + 7/3}{\gamma + 1} k(\nu) \int_{\phi_1}^{\phi_2} |B_{\perp}|^{1/2(\gamma + 1)} \frac{h}{\sin \theta \sin^2 \phi} d\phi, \tag{42}$$

$$Q = k(\nu) \int_{\phi_1}^{\phi_2} \frac{|B_{\perp}|^{1/2(\gamma+1)}}{|B_{\perp}|^2} \frac{[B_{\phi}^2 \cos^2 \phi - (B_z \sin \theta + B_{\phi} \sin \phi \cos \theta)^2]h}{\sin \theta \sin^2 \phi} d\phi, \tag{43}$$

$$U = k(\nu) \int_{\phi_1}^{\phi_2} \frac{|B_\perp|^{1/2(\gamma+1)}}{|B_\perp|^2} 2B_\phi \cos\phi (B_z \sin\theta + B_\phi \sin\phi \cos\theta) \frac{-h}{\sin\theta \sin^2\phi} d\phi,$$

where $\phi_1 = \pi \operatorname{sgn} h - \arcsin \frac{h}{R}$, $\phi_2 = \arcsin \frac{h}{R}$. It is seen that when one changes ϕ by $\pi - \phi$ the expression for U changes its sign and, therefore, U = 0. Consequently, if Q > 0 than $\tilde{\chi}_{res} = 0$, if Q < 0 then $\tilde{\chi}_{res} = \pi/2$. Thus, the electric field vector either parallel or perpendicular to the jet axis. This fact may account for the bimodal distribution of observed $\tilde{\chi}_{res}$ (Gabuzda et al., 1994a). In the case $B_z = \operatorname{constant}$, $B_\phi = B_z \Omega^F r$ and $\gamma = 3$ expressions for I and U from the unit jet length (i.e. (42) and (43) integrated over h)

$$I = \frac{\gamma + 7/3}{\gamma + 1} k(\nu) \int_{-R}^{R} dh \int_{\phi_1}^{\phi_2} |B_{\perp}|^{1/2(\gamma + 1)} \frac{h}{\sin \theta \sin^2 \phi} d\phi, \tag{44}$$

$$Q = k(\nu) \int_{-R}^{R} dh \int_{\phi_1}^{\phi_2} |B_{\perp}|^{1/2(\gamma - 3)} \frac{[\Omega^{F^2} r^2 \cos^2 \phi - (\sin \theta + \Omega^F r \sin \phi \cos \theta)^2] B_z^2 h}{\sin \theta \sin^2 \phi} d\phi, \tag{45}$$

may be reduced to the form

$$I = \frac{\gamma + 7/3}{\gamma + 1} k(\nu) B_z^{(\gamma + 1)/2} \frac{\pi}{\sin \theta} \int_0^R 2t \left[\sin^2 \theta + \Omega^{F^2} r^2(t) (1 - \frac{1}{2} \sin^2 \theta) \right] dt,$$
$$Q = k(\nu) B_z^{(\gamma + 1)/2} \pi \sin \theta \int_0^R (\Omega^{F^2} r^2(t) - 2) t dt.$$

From above we see that in the case $\gamma = 3$ the sign of Q does not depend on θ , but determined only by function $\Omega^F(t)$. For the degree of polarization

$$\Pi = \frac{\gamma + 1}{\gamma + 7/3} \sin^2 \theta \frac{\int\limits_0^R (\Omega^{F^2} r^2(t) - 2) t \, dt}{\int\limits_0^R 2t \, dt (\sin^2 \theta + \Omega^{F^2} r^2(t) (1 - \frac{1}{2} \sin^2 \theta))}.$$

In the case $\gamma=3$ and $\Omega^F=\Omega(1-(t/R)^2)$

$$\Pi = \frac{\frac{1}{2} \left(\frac{\Omega^2}{12} - 2\right)}{\sin^2 \theta + \frac{\Omega^2}{12} \left(1 - \frac{1}{2} \sin^2 \theta\right)} \frac{3}{4} \sin^2 \theta$$

If $|\Omega| > 2\sqrt{6}$, then Q > 0, $\tilde{\chi}_{res} = 0$, i.e. orientation of the magnetic field in the jet derived from observations is perpendicular to the jet axis. If $0 < |\Omega| < 2\sqrt{6}$ magnetic field looks parallel to the jet axis. Equations (44) and (45) were integrated numerically for $\Omega^F = \Omega(1 - (t/R)^2)$ and $\gamma = 2.1$, which correspond to the power law index in the spectrum of synchrotron emission of $(\gamma - 1)/2 = 0.55$, the mean observed value for extragalactic jets. Results are presented in Fig. 5. Positive values of the degree of polarization correspond to $\tilde{\chi}_{res} = 0$, negative to $\tilde{\chi}_{res} = \pi/2$. In the case $\Pi = 0$ radiation is entirely unpolarized. Note also that in nonrelativistic consideration $\Pi(180^0 - \theta) = \Pi(\theta)$ for any value of θ .

In paper Istomin & Pariev, 1996 we presented a hypothesis that knots observed in jets can be the manifestation of the "standing wave" phenomenon. If one knows the dispersion curves $\omega = \omega(k)$ and wavenumbers k_{min} at which $d\omega/dk = 0$ for perturbations one can calculate the velocity of moving crests of the "standing wave" as $v_{phas} = \omega_{min}(k_{min})/k_{min}$ and corresponding observed velocity $v_{vis} = \frac{v_{phas}\sin\theta}{1 - v_{phas}/c\cos\theta}$. Note also that changing sign of B_{ϕ} in (2) is equivalent to changing

Figure 5. Dependences of linear polarization Π on angular rotational velocity Ω (a) and on visual velocity of knots v_{vis} (b) for fundamental axisymmetric mode m=0. $\Pi>0$ when electric field vector is oriented parallel to the jet axis, $\Pi<0$ when electric field vector is oriented perpendicular to the jet axis. $v_{vis}>0$ means that observed motion of knots is direct, $v_{vis}<0$ means reversal motion. Crosses are for BL Lac objects and squares are for quasars listed in Table 1.

sign of Ω^F , since I and Q depend only on B_z and B_ϕ and not on u or E_r . On Fig. 5 we present the relationships of the polarization Π of jet emission and v_{vis} obtained in the case of Ω changing from 0 to 100 for some angles θ . We also plotted observational points for jets in BL Lac objects and quasars for which we were able to find both polarization and proper motion measurements in the literature and which are listed in Table 1. For each object we calculated degree of polarization and observed velocity as averaged over all bright knots observed in a particular object excluding a few knots peculiarity of which was indicated in original references. This pocedure might be very questionable although in the lack of observations of the emission from the space between knots on parsec scale we had nothing better. Numbers for v_{vis} were calculated assuming Hubble constant $H = 100h \text{km/s} \cdot \text{Mpc}$

In the case of accelerated particles concentrated very close to the Alfvén surface $r = r_A$ one can obtain from the expressions (44) and (45) the following formulae

$$I = \frac{\gamma + 7/3}{\gamma + 1} k(\nu) B_z^{\frac{\gamma + 1}{2}} \int_0^{2\pi} \frac{r_A}{\sin \theta} \left[\sin^2 \theta + \Omega^{F^2}(r_A) r_A^2 (1 - \sin^2 \phi \sin^2 \theta) + 2\Omega^F r_A(t) \sin \phi \cos \theta \sin \theta \right]^{\frac{\gamma + 1}{4}} d\phi,$$

$$Q = k(\nu) B_z^{\frac{\gamma + 1}{2}} \int_0^{2\pi} \frac{r_A}{\sin \theta} \left[\sin^2 \theta + \Omega^{F^2}(r_A) r_A^2 (1 - \sin^2 \phi \sin^2 \theta) + 2\Omega^F (r_A) r_A \sin \phi \cos \theta \sin \theta \right]^{\frac{\gamma - 3}{4}} \times \left(\Omega^{F^2}(r_A) r_A^2 \cos^2 \phi - (\sin \theta + \Omega^F (r_A) r_A \sin \phi \cos \theta)^2 \right) d\phi.$$

Since for axisymmetric modes (m=0) always $|\omega_{min}| > |k_{min}|$ (Istomin & Pariev, 1994) one can see from the expression (5) for A that Alfvén resonance does not exist for axisymmetric modes. Therefore, there should be no particle acceleration by this mode. The next most important modes are m=1 and m=-1. Since no one quantity k_{min} , ω_{min} or Π changes when m changes to -m and Ω^F to $-\Omega^F$, it is enough to consider only m=1 and all values of Ω^F . Polarization Π versus v_{phas} for this case is plotted in Fig. 6 as well as observational points. We showed first non-axisymmetric fundamental mode m=1 which are expected to be excited more than higher modes with m>1. Polarization curves are plotted only for values of Ω at which Alfvén resonance $r=r_A$ is present inside the jet. As previously, $\Omega^F=\Omega(1-(r/R)^2)$ and $\gamma=2.1$. It is seen that in the case of uniform particle distribution across the jet, curves for θ changing from 120° to 70° are located in the region where points from observations of BL Lac object (crosses) and quasars (squares) are situated. However, polarization curves for emitting

Table 1. Degree of polarization and velocities of knots in BL Lac objects and quasars

Class	Source	Π , $\%$	$v_{vis}h$	References
BL Lac	0454+844	25	0.6	2,3
BL Lac	0735 + 178	14.2	5.5	4,5
BL Lac	0954 + 658	17.5	5.7	1
BL Lac	1803 + 784	11.5	1.8	1
BL Lac	1823 + 568	17.75	4.05	1
BL Lac	2007 + 777	5.55	2.9	2,1
quasar,	1308 + 326	3.77	10.9	6
BL Lac?				
BL Lac	0851 + 202	6.2	2.8	7
BL Lac	1219 + 285	30	2.0	7
BL Lac	2200 + 420	10.9	3.5	7
quasar	0212 + 735	-13.35	3.9	8
quasar	0836 + 710	-31.33	7.8	8
quasar	3C279	-15.37	5.6	8
quasar	3C345	-7.	7.7	9
quasar	1928 + 738	-9.15	5.78	8
quasar	3C454.3	-15.55	8.9	8

References.— (1) Gabuzda et al. (1994a), (2) Witzel et al. (1988), (3) Gabuzda et al. (1989), (4) Båå th & Zhang (1991), (5) Gabuzda et al. (1994b), (6) Gabuzda & Cawthorne (1993), (7) Gabuzda & Cawthorne (1996), (8) private communication of Gabuzda D.C., (9) Brown, Roberts, & Wardle (1994)

Figure 6. The same plots as in Fig. 5 but emitting particles are concentrated close to the Alfvén resonance surface, m=1 fundamental mode.

particles concentrated on the Alfvén resonance surface, as it is the case if our acceleration mechanism works, do not match observation of BL Lac objects. Electric field vector is always oriented perpendicular to the jet axis.

Now let us make calculations closer to the reality taking into account Doppler boosting and presence of strong electric field. We will denote values measured in the plasma rest frame as values with primes. Let us find the transformation formulae for the polarization tensor $J_{\alpha\beta} = \langle E_{\alpha}E_{\beta}^* \rangle$ and Stocks parameters $J_{\alpha\beta} = \frac{1}{2}\begin{pmatrix} I+Q&U\\U&I-Q \end{pmatrix}$ when expressed in the source frame $x_sy_sz_s$ and the observer frame $x_oy_oz_o$. Using the transformation formulae for the electric and magnetic fields of the wave directly it is possible to obtain

$$J_{\alpha\beta o} = J'_{\alpha\beta s} \frac{1 - u^2/c^2}{(1 - u/c\cos\delta)^2}.$$
 (46)

Here we denote by δ an angle between velocity \mathbf{u} of the source and the direction towards observer \mathbf{k} measured in the observer frame, correspondently δ' is the same angle but measured in the source frame. Thus, polarization ellipse in the observer frame is obtained from polarization ellipse in the source frame by the rotation by the angle $\delta - \delta'$ in the plane containing the direction

to the observer ${\bf n}$ and ${\bf u}$. Therefore the degree of polarization is not changed. Since for one particle Stocks parameters are expressed through the radiation flux with two main directions of polarization $p_{\nu'}^{(1)}$ and $p_{\nu'}^{(2)}$ by the formulae $I=p_{\nu'}^{(1)}+p_{\nu'}^{(2)}$, $Q=(p_{\nu'}^{(1)}-p_{\nu'}^{(2)})\cos 2\tilde{\chi}$, $U=(p_{\nu'}^{(1)}-p_{\nu'}^{(2)})\sin 2\tilde{\chi}$ then $p_{\nu}^{(1)}$ and $p_{\nu}^{(2)}$ are transformed as $p_{\nu}^{(1)}=p_{\nu'}^{(1)}\frac{d\nu'}{d\nu}\frac{1-u^2/c^2}{(1-u/c\cos\delta)^2}$, $p_{\nu}^{(2)}=p_{\nu'}^{(2)}\frac{d\nu'}{d\nu}\frac{1-u^2/c^2}{(1-u/c\cos\delta)^2}$. Therefore the intensity

$$I(\nu, \mathbf{k}) = \int (p_{\nu'}^{(1)}(\nu', \mathcal{E}', \mathbf{R}, \chi', \psi') + p_{\nu'}^{(1)}(\nu', \mathcal{E}', \mathbf{R}, \chi', \psi')) \times \frac{d\nu'}{d\nu} \frac{1 - u^2/c^2}{(1 - u/c\cos\delta)^2} K_e \mathcal{E}'^{-\gamma} \frac{dV'}{dV} d\mathcal{E}' d\Omega_{\tau'} R^2 dR,$$

where χ' is an angle between momentum of the particle and the magnetic field vector, ψ' is the angle between the direction of radiation and the cone formed by rotating velocity vector, both measured in the frame comoving with the fluid element. We will make integration over momenta in the plasma rest frame while integration over space coordinates in the observer frame. Integration over solid angle $\Omega_{\tau'}$ in the momenta space may be done analogous to the usual case of synchrotron emission of ultra-relativistic particles, when there is no electric field $\mathbf{E} = -\mathbf{u} \times \mathbf{B}$. Integration over \mathcal{E}' leads to (see, e.g., Ginzburg, 1989)

$$I(\nu, \mathbf{k}) = \frac{\gamma + 7/3}{\gamma + 1} k(\nu) \int \left(\frac{1 - u/c \cos \delta}{\sqrt{1 - u^2/c^2}} \right)^{-\frac{\gamma - 1}{2}} (B' \sin \chi')^{\frac{\gamma + 1}{2}} \frac{dR}{1 - u/c \cos \delta}$$
(47)

Here $\nu' = \nu \frac{1 - u/c\cos\delta}{\sqrt{1 - u^2/c^2}}$, δ is the angle between **u** and the direction to the observer, χ' is the angle between the magnetic

field in the plasma rest frame \mathbf{B}' and the line of sight, integration is performed along the line of sight. The expressions for Q and U are obtained in the same fashion.

$$Q(\nu, \mathbf{k}) = k(\nu) \int \left(\frac{1 - u/c \cos \delta}{\sqrt{1 - u^2/c^2}} \right)^{-\frac{\gamma - 1}{2}} (B' \sin \chi')^{\frac{\gamma + 1}{2}} \frac{\cos 2\tilde{\chi} dR}{1 - u/c \cos \delta},$$

$$U(\nu, \mathbf{k}) = k(\nu) \int \left(\frac{1 - u/c \cos \delta}{\sqrt{1 - u^2/c^2}} \right)^{-\frac{\gamma - 1}{2}} (B' \sin \chi')^{\frac{\gamma + 1}{2}} \frac{\sin 2\tilde{\chi} dR}{1 - u/c \cos \delta}.$$

Using the transformation rules leads us to the expression for the $B' \sin \chi'$

$$B'^2 \sin^2 \chi' = B_\phi^2 + B_z^2 - E_r^2 -$$

$$\frac{[-E_r(1-u^2)(u_z\sin\phi\sin\theta + u_\phi\cos\theta) + u(\cos\delta - u)(u_\phi B_\phi + u_z B_z)]^2}{u^4(1-u\cos\delta)^2}$$
(48)

and using of (46) gives us the expression for $\tilde{\chi}$

$$\tilde{\chi} = \tilde{\chi}_u + \sigma,\tag{49}$$

$$\tan \tilde{\chi}_v = \frac{E_r(u^2 - u\cos\delta)(u_z\sin\phi\sin\theta + u_\phi\cos\theta) - u^2\sin^2\delta(u_\phi B_\phi + u_z B_z)}{E_r u^2\sin\theta\cos\phi(1 - u\cos\delta)}$$

$$0 < \tilde{\chi}_u < \pi$$

$$\cos \sigma = -\frac{u_{\phi} \sin \phi \cos \theta + u_z \sin \theta}{u \sin \delta}, \quad \sin \sigma = -\frac{u_{\phi} \cos \phi}{u \sin \delta},$$

 $u\cos\delta = -\sin\theta\sin\phi u_{\phi} + \cos\theta u_{z}$

Assuming uniform particle distribution for the emission from the unit length we obtain

$$I = \frac{\gamma + 7/3}{\gamma + 1} \frac{k(\nu)}{\sin \theta} \int_{0}^{R} r \, dr \int_{0}^{2\pi} d\phi \left(\frac{1 - u \cos \delta}{\sqrt{1 - u^{2}}} \right)^{-\frac{\gamma - 1}{2}} \frac{|B' \sin \chi'|^{(\gamma + 1)/2}}{1 - u \cos \delta}$$

$$Q = \frac{k(\nu)}{\sin \theta} \int_{0}^{R} r \, dr \int_{0}^{2\pi} d\phi \left(\frac{1 - u \cos \delta}{\sqrt{1 - u^{2}}} \right)^{-\frac{\gamma - 1}{2}} |B' \sin \chi'|^{(\gamma + 1)/2} \frac{\cos 2\tilde{\chi}}{1 - u \cos \delta}$$

$$U = \frac{k(\nu)}{\sin \theta} \int_{0}^{R} r \, dr \int_{0}^{2\pi} d\phi \left(\frac{1 - u \cos \delta}{\sqrt{1 - u^{2}}} \right)^{-\frac{\gamma - 1}{2}} |B' \sin \chi'|^{(\gamma + 1)/2} \frac{\sin 2\tilde{\chi}}{1 - u \cos \delta}.$$
(50)

Figure 7. Dependences of polarization Π on Ω (a), on v_{vis} for $\gamma=2.1$ (b) and for $\gamma=3$. (c). Emitting particles are concentrated close to the Alfvén resonant surface. Here $B_{\phi}=+\Omega^F r B_z$, fundamental eigenmode with m=1. Notations are the same as in Fig. 5. In Fig. (a) solid curves are for $\gamma=2.1$, dashed are for $\gamma=3$.

Assuming particles to be located close to the Alfvén resonance surface in the region $|r - r_A| \leq \Delta$ and $\Delta \ll R$ we have

$$I = \frac{\gamma + 7/3}{\gamma + 1} \frac{k(\nu)}{\sin \theta} \Delta \int_{0}^{2\pi} d\phi r_{A} \left(\frac{1 - u \cos \delta}{\sqrt{1 - u^{2}}}\right)^{-\frac{\gamma - 1}{2}} \frac{|B' \sin \chi'|^{(\gamma + 1)/2}}{1 - u \cos \delta}$$

$$Q = \frac{k(\nu)}{\sin \theta} \Delta \int_{0}^{2\pi} d\phi r_{A} \left(\frac{1 - u \cos \delta}{\sqrt{1 - u^{2}}}\right)^{-\frac{\gamma - 1}{2}} \times$$

$$|B' \sin \chi'|^{(\gamma + 1)/2} \frac{\cos 2\tilde{\chi}}{1 - u \cos \delta}$$

$$U = \frac{k(\nu)}{\sin \theta} \Delta \int_{0}^{2\pi} d\phi r_{A} \left(\frac{1 - u \cos \delta}{\sqrt{1 - u^{2}}}\right)^{-\frac{\gamma - 1}{2}} \times$$

$$|B' \sin \chi'|^{(\gamma + 1)/2} \frac{\sin 2\tilde{\chi}}{1 - u \cos \delta}.$$
(51)

In the force—free approach constant K determining the component of \mathbf{u} parallel to the magnetic field in the observer frame \mathbf{B} remains to be free. We choose it such that the velocity \mathbf{u} of plasma has the least possible absolute value for a given B_z and $\Omega^F r$. This choice is the same as in (3) $u_z = -\frac{B_\phi B_z}{B_\phi^2 + B_z^2} \Omega^F r$, $u_\phi = -\frac{B_z^2}{B_\phi^2 + B_z^2} \Omega^F r$ for the value of K equals to the $-\Omega^F r B_\phi/B^2$. It can be checked that under change of ϕ to $-\phi$ the value of Q is not changed, and the sign of U is reversed. Thus, as a result of integration U=0 and either $\tilde{\chi}_{res}=0$ or $\tilde{\chi}_{res}=\pi/2$ as it is when we do not take into account Doppler boosting and electric field.

We performed numerical calculations according to (50) and (51) using (48) and (49). As above we take $B_z = \text{constant}$, $\Omega^F = \Omega(1 - (r/R)^2)$, $B_\phi = \pm \Omega^F r B_z$. Results for uniform particle distribution do not match observations. Taking into account presence of the electric field and Doppler boosting changes the polarization of synchrotron emission essentially. Now only for small values of angle θ and high Ω apparent direction of the magnetic field as it is usually derived from polarization measurements (just perpendicular to the electric vector in the polarized component of the radiation) is transversal to the jet axis. For most of inclination angles θ and angular velocities Ω apparent magnetic field is longitudinal. One can also see from Fig. 7, where we plotted Π versus v_{vis} for $B_\phi = +\Omega^F r B_z$, that our simulation does not match observational data. However,

Figure 8. Dependences of polarization Π on Ω (a), on v_{vis} for $\gamma=2.1$ (b) and for $\gamma=3$. (c). Emitting particles are concentrated close to the Alfvén resonant surface. $B_{\phi}=-\Omega^F r B_z$, fundamental eigenmode with m=1 Notations are the same as in Fig. 5. In Fig. (a) solid curves are for $\gamma=2.1$, dashed are for $\gamma=3$.

for $B_{\phi} = -\Omega^F r B_z$ we are able to reproduce observations well enough, if particles are distributed close to the Alfvén surface and m = 1 or m = -1. As for the case without Doppler boosting effect and without taking account electric field, Π is not changed when one changes the sign of Ω , but Π is changed when one put $B_{\phi} = -\Omega^F r B_z$ instead of $B_{\phi} = \Omega^F r B_z$. Let us list all transformations which do not change equations for radial modes (5) or lead to complex conjugated equations for ξ^* :

```
(i) \omega \to -\omega^*, k \to -k, \Omega \to -\Omega;

(ii) \omega \to -\omega^*, k \to -k, m \to -m;

(iii) \Omega \to -\Omega, m \to -m;

(iv) k \to -k, B_{\phi} = +\Omega^F r B_z \to B_{\phi} = -\Omega^F r B_z;

(v) B_z \to -B_z.
```

So, if one set of parameters satisfies equations (5) than parameters with changed signs will also satisfy equations (5) for the same ξ or for ξ^* . Obviously, these substitutions are valid for k_{min} and ω_{min} as well. The value of r_A also is not changed under transformations listed above. Degree of polarization Π is not influenced by changing sign of B_z as well as by changing sign of Ω . The crucial fact is that changing sign in relation $B_{\phi} = \pm \Omega^F r B_z$ leads to changing sign of $v_{phas} = \omega_{min}/k_{min}$, whilst all other four transformations change neither Π nor they change v_{phas} . Therefore, in the sense of correlation between Π and v_{vis} , which can be verified experimentally, all different cases are reduced to considering both signs in the relation $B_{\phi} = \pm \Omega^F r B_z$, but we can restrict ourself to $B_z > 0$, m > 0 and all Ω for which r_A is located inside the jet. Using formulae (48), (49), (50) and expressions (3) for u_z and u_{ϕ} one can check that Stocks parameters remain unchanged when one changes sign of B_{ϕ} and replace angle θ by $\pi - \theta$. Also, simultaneous changing of sign of v_{phas} and θ to $\pi - \theta$ leads to that v_{vis} is transformed into $-v_{vis}$. Therefore, dependences of Π on v_{vis} in the case $B_{\phi} = -\Omega^F r B_z$ can be obtained from same dependences in the case $B_{\phi} = +\Omega^F r B_z$ by reflection $v_{vis} \to -v_{vis}$ and relabelling each curve from θ to $\pi - \theta$.

We plotted degree of linear polarization Π versus v_{vis} for m=1 in Figs. 7 and 8 for $B_{\phi}=+\Omega^F r B_z$ and $B_{\phi}=-\Omega^F r B_z$ correspondently. Alfvén resonance exists for $0.7 < \Omega < 4.9$. Therefore, along curves in Figs. 7 and 8 the value of Ω changes in this interval. We see that curves in Fig. 7 do not match observational data for knots in jets, while those in Fig. 8 do. Dependence on the power law index γ of emitting particles is small. We plotted results for $\gamma = 2.1$ and $\gamma = 3$. which are maximum and minimum values of γ obtained in the process of the formation of the spectrum (see section 3).

We can suggest the following explanation of the fact that knots in jets with $B_{\phi} = -\Omega^F r B_z$ are observed more often than in jets having the opposite winding of the magnetic field. If we look at the models of the formation of magnetically driven jets from accretion discs (see, e.g. Pelletier & Pudritz, 1992) we will find that magnetic field lines are always bent in the direction

opposite to the direction of disc rotation as soon as the velocity of the outflow is directed outwards from the disc plane. This means that in the jet approaching the observer $B_{\phi} = -\Omega^F r B_z$, whilst in the jet receding from the observer $B_{\phi} = + \Omega^F r B_z$. Disturbances propagating along approaching jet should be brighter than those in the counter-jet due to the Doppler boosting effect. Therefore, we will observe knots in parts of jets having $B_{\phi} = -\Omega^F r B_z$ more often than in those with $B_{\phi} = +\Omega^F r B_z$. This explains the fact that the number of sources having $\Pi > 0$ is approximately the same as the number of sources having $\Pi < 0$ despite that for most of the values of parameters calculations give longitudinal polarization $\Pi < 0$. Also the difference between jets in BL Lac objects and jets in quasars finds its explanation by systematically different values of Ω^F . In the frame of our model jets in BL Lac objects have higher value of Ω^F than jets in quasars. Although we performed calculations only for one particular profile of $\Omega^F(r)$ which seems to be close to what one should obtain from theory of the formation of jets (Istomin & Pariev, 1996) we found this tendency and it should be general for profiles of $\Omega^F(r)$ which are qualitively similar to chosen one. There are many physical arguments though (Istomin & Pariev, 1994; Istomin & Pariev, 1996; Beskin, Istomin & Pariev, 1992a), why the real dependence $\Omega^F(r)$ should have qualitative properties similar to $\Omega(1 - (r/R)^2)$ that we chose in our computations.

5 SUMMARY

In present work we considered possible acceleration of electrons and positrons inside relativistic rotating electron-positron force-free cylindrical jet with spiral magnetic field. It is very plausible that inner parsec-scale jets in active galaxies can be described in the frame of this physical model. The observations of jets in 3C273 and M87 points out that the extragalactic jets are most probably electron-positron rather than electron-proton (Morrison & Sadun, 1992; Reynolds et al., 1996) Also it seems to be very likely that such jets are not in steady state and contain waves excited by environmental processes, of which most powerful would be the variability of accretion rate onto central black hole and accretion disc instabilities both strongly perturbing magnetic field at the base of the jet. We considered the behaviour of such excitations inside cylindrical force-free jet in our previous works (Istomin & Pariev, 1994; Istomin & Pariev, 1996) and found that in wide range of parameters determining the equilibrium structure of electromagnetic fields and perturbations inside the jet there exist resonant surfaces on which the phase speed of eigenmodes is equal to local Alfvén velocity. Those eigenmodes for which there is an Alfvén resonance occured to have small damping decrement, whilst those having no Alfvén resonances are neutrally stable. This fact points that existence of Alfvén resonance leads to losses of energy of corresponding eigenmodes. In present work we found how particles are accelerated in the strong fields near the Alfvén surface. Acceleration process and synchrotron losses combined together form power law energy spectrum of ultra-relativistic electrons and positrons with index between 2 and 3 depending upon initial energy of injected particles. The power law spectrum goes up to the energy \mathcal{E}_{max} , where the sharp fall down occurs (see Figs. 2,3). The magnitude of \mathcal{E}_{max} depends on the initial particle temperature T_0 as well as on the characteristic acceleration energy $\mathcal{E}_1(26)$, $\mathcal{E}_{max} \approx \mathcal{E}_1/\ln(\mathcal{E}_1/T_0)$. The quantity of T_0 evaluated from the equipartition condition in the acceleration region is equal to 10 MeV for the quantities of magnetic field and density 10⁻²G and 0.1cm⁻³ correspondingly. As to the quantity of \mathcal{E}_1 , it is, in accordance with (26), of the order of $10^4 (\delta B/B_0)^2 \text{MeV}$ for the same value of B_0 , where $\delta B/B_0$ is the dimensionless amplitude of the perturbation. For large perturbations ($\delta B \approx B_0$) \mathcal{E}_1 reaches the values of the order of 10^3 MeV. Thus particles accelerated near Alfvén resonance are in the energy range of 10MeV $< \mathcal{E} < 10^3$ MeV. These particles emitt synchrotron radiation in the range of frequences approximately from 1MHz to 100GHz which covers the frequences of modern radio observations.

In order to obtain observable predictions of our theory of standing wave excitations inside jets, we computed synchrotron radiation emitted by accelerated particles. We considered two possibilities: 1) ultra-relativistic particles distributed uniformly across the jet, 2) ultra-relativistic particles concentrated close to the Alfvén resonance surface. The latter distribution follows from our acceleration theory and we compared it with the former one which might be produced by other acceleration processes. We assumed uniform magnetic field in the jet, so the equilibrium configuration of the jet is determined only by the radial profile of angular rotational velocity $\Omega^F(r)$ of magnetic field lines. In our computations we also specified component of the velocity parallel to the magnetic field lines in a way to minimize the kinetic energy associated with the flow and took $\Omega^F(r) = \Omega(1 - (r/R_{jet})^2)$. The actual velocity is determined by the processes of jet formation which is poorly understood now, still such minimal velocity is physically favoured (Novikov & Frolov, 1986). The prominent characteristic of synchrotron radiation is its polarization: degree of linear polarization and orientation of electric vector with respect to the jet axis. We calculated these quantities for the emission integrated over the jet cross section taking into account relativistic bulk spiral flow of plasma in the jet, which leads to the presence of electric field comparable by magnitude with the magnetic field, Doppler boosting effect for the intensity of synchrotron radiation and swing of the polarization position angle. We want to stress that the last effect, which was first pointed out for the simpler case of uniform magnetic field parallel to the jet axis by Blandford & Königl in 1979, substantially modifies resulting degree of linear polarization from the whole jet. However, because of the axial symmetry of the problem, only two orientations of polarization position angle are possible: parallel or perpendicular with respect to the jet axis. Observations of polarization of VLBI scale jets (Gabuzda et al., 1994a) also show

bimodal distribution of the position angle: most of knots in BL Lac objects and quasars have polarization either close to the jet axis or perpendicular to it.

We also calculated velocities of crests of standing eigenmodes and compared them with the observed proper motions of bright VLBI knots in jets. We were able to match observational data only for the case when emitting particles are concentrated close to the Alfvén resonance surface and magnetic field lines are twisted in the direction opposite to the direction of rotation Ω^F . The last fact can be understood by selection effect due to the Doppler boosting which makes sources with jets approaching the observer more favourable observed than receding jets. Comparing calculations with observations we can estimate angular rotational velocity of jets. We obtained that Ω^F in BL Lac objects is intrinsically larger than in quasars which accounts for the difference in polarization properties of these two classes of objects (Gabuzda et al., 1994a): in BL Lac the magnetic field inferred from polarization position angle is oriented predominantly perpendicular to the jet axis, in quasars it is parallel to the jet axis.

Acknowledgments

Authors are grateful to Gabuzda D.C. for compiling observational data on polarization of quasars and helpful discussions of different observational issues. This work was done under the partial support of the Russian Foundation for Fundamental Research (grant number 96-02-18203) VIP acknowledges also partial support from European Southern Observatory within the C& EE Programme.

References

Appl S., Camenzind M., 1992, A&A, 256, 354

Båå th L.B., Zhang F.J., 1991, A&A, 243, 328

Begelman M.C., Blanford R.D. & Rees M.J. 1984, Rev. Mod. Phys., 56, 255

Beskin V.S., Istomin Ya.N., Pariev V.I., 1992a, in the book Extragalactic Radio Sources — From Beams to Jets, edited by J. Roland, H. Sol, G. Pelletier. Cambridge University Press, Cambridge

Beskin V.S., Istomin Ya.N., Pariev V.I., 1992b, AZh, 69, 1258

Blandford R.D., Königl A., 1979, ApJ, 232, 34

Blanford R.D., Pringle J.E., 1976, MNRAS, 176, 443

Brown L.F., Roberts D.H., Wardle J.F.C., 1994, ApJ, 437, 108

Gabuzda D.C., Cawthorne T.V., 1993, in Davis R.J., Booth R.S., eds, Subarcsecond Radio Astronomy. Cambridge Univ. Press, Cambridge, p.211

Gabuzda D.C., Cawthorne T.V., 1996, MNRAS, 283, 759

Gabuzda D.C., Cawthorne T.V., Roberts D.H., Wardle J.F.C., 1989, ApJ, 347, 701

Gabuzda D.C., Mullan C.M., Cawthorne T.V., Wardle J.F.C., Roberts D.H., 1994a, ApJ, 435, 140

Gabuzda D.C., Wardle J.F.C., Roberts D.H., Aller M.F., Aller H.D., 1994b, ApJ, 435, 128

Ginzburg V.L., 1989, Applications of Electrodynamics in Theoretical Physics and Astrophysics. Gordon and Breach Science Publishers, New York, p.65

Istomin Ya.N., Pariev V.I., 1994, MNRAS, 267, 629

Istomin Ya.N., Pariev V.I., 1996, MNRAS, 281, 1

Mikhaylovskii A.B., 1975, in Reviews of Plasma Physics, ed. by Leontovich H.A., Consultants Bureau, New York, Vol.6, p.77 Morrison P., Sadun A., 1992, MNRAS, 254, 488.

Mushotzky R.F., Done C., Pound K., 1993, Ann. Rev. Astron. Astrophys., 717

Novikov I.D., Frolov V.P., 1986, The Physics of Black Holes. Nauka Press, Moscow

Pelletier G., Pudritz R., 1992, ApJ, 394, 117

Rees M.J., 1984, Ann. Rev. Astron. Astrophys. ,471

Reynolds C.S., Fabian A.C., Celotti A., Rees M.J., 1996, MNRAS, 283, 873.

Sivukhin D.V., 1965, in Reviews of Plasma Physics, ed. by Leontovich H.A., Consultants Bureau, New York, Vol.1, p.1

Torricelli-Ciamponi G., Petrini P., 1990, ApJ., 361, 32

Witzel A., Schalinski C.J., Johnston K.J., Biermann P.L., Krichbaum T.P., Hummel C.A., Eckart A., 1988, A&A, 206, 245 Witzel A., Wagner S., Wegner R., Steffen W., Kirchbaum T., 1993, in Davis R.J. & Booth R.S., eds Sub-arcsecond Radio Astronomy. Cambridge Univ. Press, Cambridge, p. 159

